Available online at www.sciencedirect.com
SCIENCE DIRECT
Journal of Photochemistry and Photobiology A: Chemistry 173 (2005) 340–348
Journal of Photochemistry and Photobiology A:Chemistry
www.elsevier.com/locate/jphotochem

Chiral discrimination in the complexation of heptakis-(2,6-di-*O*-methyl)-β-cyclodextrin with 2,3-diazabicyclo[2.2.2]oct-2-ene derivatives

Hüseyin Bakirci, Werner M. Nau *

School of Engineering and Science, International University Bremen, Campus Ring 1, D-28759 Bremen, Germany

Available online 23 May 2005

Abstract

The chiral discrimination of enantiomeric camphanate esters of 2,3-diazabicyclo[2.2.2]oct-2-ene by heptakis-(2,6-di-*O*-methyl)-β-cyclodextrin was studied by means of induced circular dichroism, UV spectrophotometry, and fluorescence spectroscopy. The first two spectroscopic techniques were employed to study the thermodynamics, while the kinetics of complexation was determined by using steady-state fluorescence quenching experiments. The formation of 1:1 and 2:1 inclusion complexes was monitored through opposite induced circular dichroism effects and an increase of the near-UV extinction coefficient of the azo chromophore, from which the binding constants (*K*) were determined by means of titrations. The binding constants for 1:1 complexation (ca. 1500 M^{-1}) were more than 1 order of magnitude larger than those for 2:1 complexation (ca. 40 M^{-1}). An insignificant chiral discrimination was found for the thermodynamics of 1:1 complexation, but a significant effect on the association kinetics, which was ca. 20% faster for the (−)-enantiomer. The association rate constants for the formation of the 2:1 complex were found to be too small (<1×10^7 s^{-1}) to allow determination by the fluorescence quenching method.

Keywords: Chiral discrimination; Cyclodextrins; Fluorescence; Circular dichroism; Host–guest complexes

1. Introduction

Cyclodextrins (CDs) are water-soluble, naturally occurring container-type host molecules, which are able to include a variety of guest molecules [1]. Their host–guest complexation behavior has been studied in great detail [2,3], which has assisted the development of applications in biomimetics [4], photochemistry [5], drug discovery [6], catalysis [7], and analytical techniques [8]. Owing to their natural occurrence as a single enantiomeric form, their complexation with racemic guests leads to the formation of diastereomeric complexes displaying different physical properties. For example, the complexes display different chemical shifts, which has enabled the use of CDs as chiral shift reagents in NMR spectroscopy [9,10].

Structural differences between diastereomeric CD complexes have been analyzed in detail from crystallographic data in the solid state [11], while induced circular dichroism, which has been frequently employed for structural assignments of CD complexes in solution [12–14], has been less frequently employed to study structural differences in diastereomeric CD complexes. Thermodynamic data are more readily accessible, including binding constants for diastereomeric complexes [3]. Temperature-dependent measurements or, preferably, isothermal titration calorimetry, have afforded insights into enthalpic versus entropic factors, which has been used to track the origin of the enantioselectivity for the complexation of chiral guests with CDs [15]. Note that different binding constants of enantiomers enable the use of CDs as chiral selectors in chromatography-based separation techniques [8]. In contrast to thermodynamic differences of diastereomeric host–guest complexes, differences in the complexation kinetics (rate constants for association and dissociation) have been rarely considered, although they could be equally important in applications relying on reversible, dynamic processes like those found in chromatography for the exchange between stationary phase and analyte, for catal-

* Corresponding author. Tel.: +49 421 200 3233; fax: +49 421 200 3229.
E-mail address: w.nau@iu-bremen.de (W.M. Nau).

1010-6030/$ – see front matter © 2005 Elsevier B.V. All rights reserved.
doi:10.1016/j.jphotochem.2005.04.019

ysis, transport phenomena, and in regulated drug delivery [16–19].

One intrinsic problem related to studying the kinetics of CD complexation (association and dissociation rate constants) is related to the fast nanosecond time scale on which these elementary processes occur [20,21]. The fast time-resolved techniques, which have been employed so far to investigate the kinetics of CD complexation in the nanosecond time domain are temperature-jump [22], ultrasonic relaxation [23], direct experiments based on time-resolved triplet quenching [24–26] or time-resolved as well as steady-state fluorescence quenching [17,18], and indirect external quencher experiments [16,19,27]. Alternatively, indirect techniques are based on NMR coalescence or spin exchange spectroscopy (slow kinetics) [28,29], or on EPR coalescence (faster kinetics) [30,31]. Stopped-flow methods have also been applied in some cases [32–34].

Nowadays, there is an agreement that the association rate constants of uncharged polar as well as nonpolar guest molecules are on the order of 10^8–$10^9\ M^{-1}\ s^{-1}$, typically about a factor of 10 below the diffusion-controlled rate, if the guest molecules are sufficiently small to form tight inclusion complexes with the selected CD [16–19,23–27,31]. Slower rates may apply if the selected CD is small (mostly for α-CD) and the selected guest is too large [22,32,33], or if higher order (2:1 and 2:2) complexes are formed [34]. Substantially slower rate constants have been reported in the literature, and in some cases it is not clear whether the slow rate constants are real, e.g., due to the presence of charges [28,29,32], whether they are related to the model-dependent indirect data analysis [30], or whether they report on a secondary relocation reaction involving pre-equilibria rather than on the elementary process of primary association [32,33]. The dissociation rate constants show naturally a larger variation [18,19], since they depend inversely on the binding affinity of the guests, which shows five orders of magnitude variation among different guests ($K = 1\ M^{-1}$ to $K = 10^5\ M^{-1}$) [2,35].

We have recently introduced the azoalkane 2,3-diazabicyclo[2.2.2]oct-2-ene (DBO) as a new versatile probe for assessing supramolecular complexation phenomena [17]. In addition to its high water solubility and non-aromaticity, which differenciates it from traditional photophysical probes [21,36], DBO is accessible by near-UV absorption and induced circular dichroism as well as fluorescence spectroscopy [13,17,18,37,38]. While the first two techniques, along with ^{1}H NMR, allow reliable assessments of the thermodynamics of complexation, its exceedingly long-lived fluorescence (505 ns in aerated D_2O) [18] has been used to probe the kinetics of complexation with CDs by time-resolved as well as steady-state fluorescence quenching [17,18]. In addition, the induced circular dichroism effects have been employed to determine the co-conformations of the host–guest complexes in solution [13,37,39], i.e., the relative coformation of the host to the guest inside the CD cavity [40].

In this work, we choose the (+)/(−)-camphanate esters of 2,3-diazabicyclo[2.2.2]oct-2-ene (**1**) as enantiomeric guest molecules to investigate chiral discrimination by UV absorption, induced circular dichroism, and fluorescence spectroscopy in the search for overarching relationships between structural, thermodynamic, and kinetic aspects of the molecular recognition process. While the DBO chromophore served mainly as photophysical probe, the camphanate moiety was selected as chiral auxiliary, since camphor and its derivatives have been shown to be responsive to chiral discrimination by CDs [15,41]. In the present study, chiral discrimination of the kinetics of CD complex formation was of particular interest, since a previous approach toward this goal was not successful [16]. Amongst the various CDs with different sizes, β-CD was selected, which shows the highest binding constant with the DBO probe [17]. Preliminary experiments were performed with natural β-CD as host, but this complexation was complicated by precipitation of the 2:1 complex, which is described separately [38]; the synthesis of the chiral esters **1** has also been documented in this context. Herein, instead of the natural β-CD, the derivative heptakis-(2,6-di-*O*-methyl)-β-cyclodextrin (DMe-β-CD) was employed, in which the 2-OH and 6-OH groups are methylated, see structure below. DMe-β-CD is also better water-soluble than β-CD, which suppressed precipitation of its complexes with **1** and allowed additionally the use of higher host concentrations, e.g., to more reliably determine higher-order equilibria.

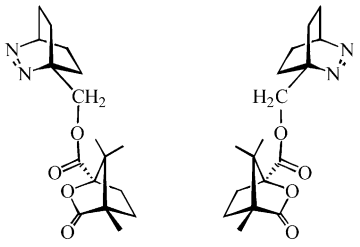

1*R*-(+)-**1** 1*S*-(−)-**1**

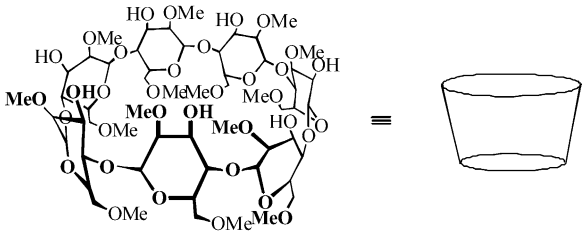

DMe-β-CD

2. Experimental details

2.1. Materials

DMe-β-CD (> 98%) was purchased from Fluka and used without further purification. The esters **1** were prepared from the hydroxymethyl derivative of DBO and the camphanic acid chlorides in enantiopure form as previously described [38]. All measurements were performed in aerated D_2O (Glaser AG, Basel, Switzerland, >99%).

2.2. Spectroscopic measurements

Circular dichroism spectra were recorded with a Jasco J-810 circular dichrograph (0.1 nm resolution, 5 accumulations) with reference to a D_2O solution containing the same host concentration, but without added guest. UV spectra were obtained with a Varian Cary 4000 spectrophotometer (0.1 nm resolution). Corrected steady-state fluorescence spectra were measured with a Varian Cary Eclipse fluorometer. Steady-state fluorescence quenching experiments with DMe-β-CD were performed with excitation at 367 nm, near the isosbestic point between free DBO and its 1:1 complexes. All titration experiments were performed in conventional 4-ml Hellma fluorescence quartz cells (light path 10 mm) by using 2.5 ml of a solution containing 0.5–2 mM guest and successively adding solid host (0.1–50 mM).

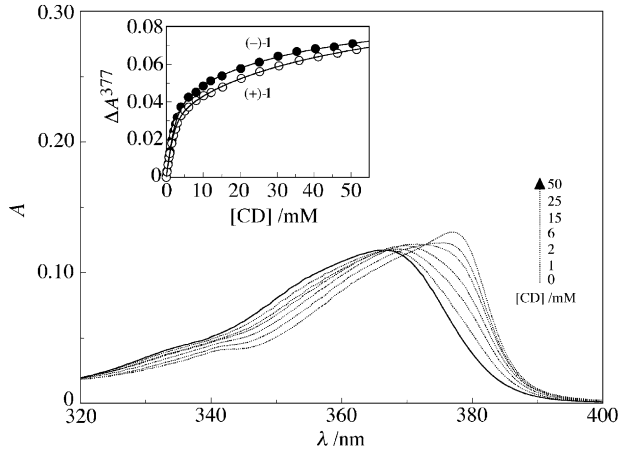

Fig. 1. Absorption spectra of (−)-**1** (2 mM) in D_2O at various concentrations of DMe-β-CD. The inset shows the UV absorption titration plots at λ_{max} = 377 nm according to Eq. (1a).

3. Results and discussion

3.1. UV absorption measurements

The effect of the addition of DMe-β-CD on the UV absorption spectra of **1** was studied in the wavelength range between 300 and 400 nm by keeping the concentration of **1** constant at 2 mM and varying the concentration of DMe-β-CD from 0.2 to 50 mM. As a typical example of the observed spectral change with the addition of host, the UV spectra of the (−)-enantiomer at various DMe-β-CD concentrations are shown in Fig. 1. In the presence of DMe-β-CD, the absorption maximum of the azo chromophore (λ_{max} = 366 nm, $\varepsilon = 57\ M^{-1}\ cm^{-1}$) undergoes a batho- and hyperchromic shift (λ_{max} = 377 nm, $\varepsilon = 77\ M^{-1}\ cm^{-1}$ at 50 mM DMe-β-CD). The well-defined isosbestic points at about 367 nm (at low host concentration) and 373 nm (at high host concentration) are indicative of a three-state equilibrium with sequential complexation and significant differences in the binding constants. This can be assigned to the initial formation of a 1:1 complex at low concentration followed by the formation of a 1:2 complex at higher concentration (Scheme 1, lower reaction sequence). The binding constant for 2:1 complexa-

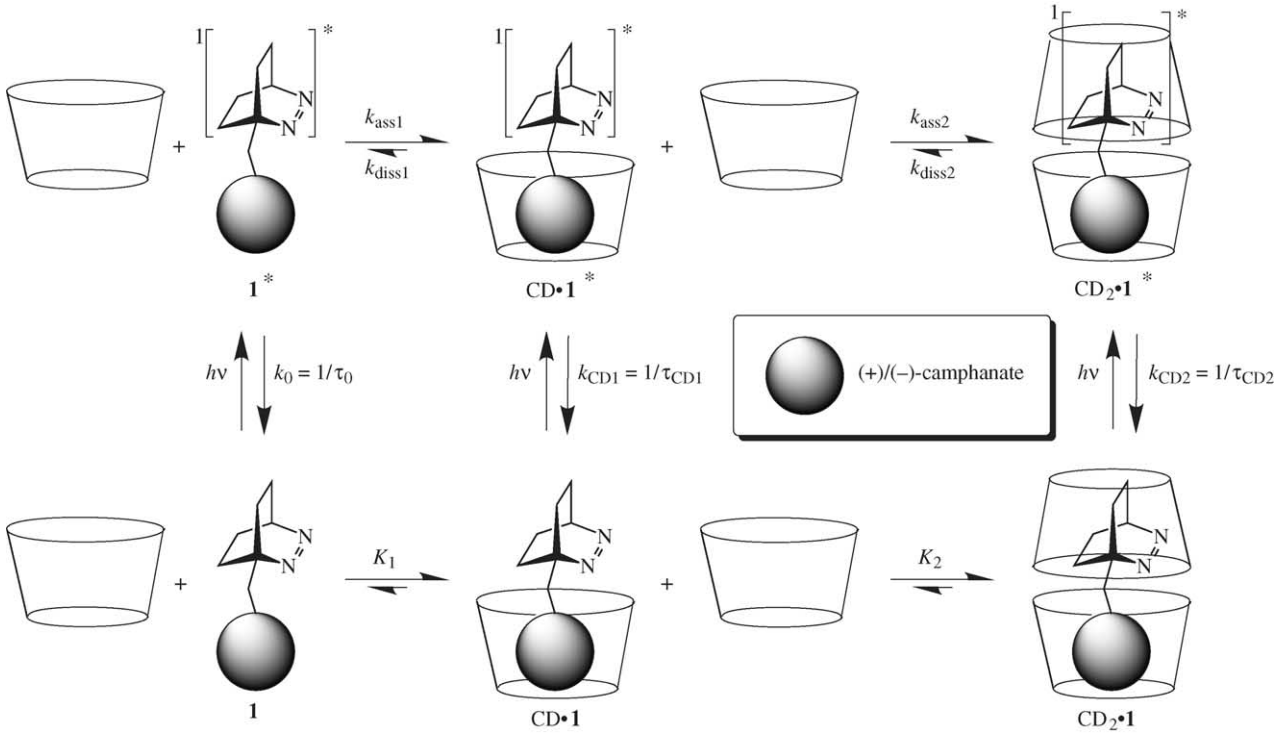

Scheme 1.

tion (K_2) must therefore be substantially smaller than for 1:1 complexation (K_1); otherwise, the isosbestic points would be less well-defined or absent. Very similar behavior with minor spectral differences was found for the (+)-enantiomer.

In Scheme 1, we assume that the camphanate moiety of **1** is preferentially included in the 1:1 complex, and that the second host molecule subsequently caps the DBO part. This sequence appears reasonable on the basis of the binding constants, which were found to be larger for the respective model compounds (ca. 1200 M^{-1} for (+)/(−)-ethyl camphanate and 320 M^{-1} for acetylated 1-hydroxymethyl–DBO) [38], and is also supported by the spectroscopic data, which suggest a greatly altered microenvironment for the DBO chromophore in the 1:2 versus the 1:1 complex, e.g., a larger bathochromic shift.

The absorption-spectral response of the DBO chromophore to the environment is well understood [42,43]. Accordingly, the bathochromic shift upon addition of DMe-β-CD, which is accompanied by an enhanced oscillator strength (increase by 15%) can be related to an increased polarizability (*P*), which the DBO chromophore experiences inside the 2:1 inclusion complex [42]. A value of $P = 0.235 \pm 0.005$ can be extrapolated to conditions of quantitative complexation, which is somewhat larger than the polarizability found inside 1:1 complexes ($P = 0.204$) [43], in line with the better protection from the aqueous bulk.

3.2. Circular dichroism and induced circular dichroism measurements

The circular dichroism spectra of both enantiomers in the absence of DMe-β-CD (Fig. 2) display a virtually perfect mirror–image relationship, which confirms the purity of the newly synthesized samples in general, and their enantiomeric purity in particular. There are two circular dichroism bands centered at 226 nm and a weaker one at 370 nm. The former is related to the n, π* Cotton effect of the carboxyl group, while the latter is characteristic for the n⊥,π* transition of the azo chromophore [13,39]. Note that the azo transition responds quite strongly with respect to its chiro-optic properties to the remotely tethered chiral auxiliary.

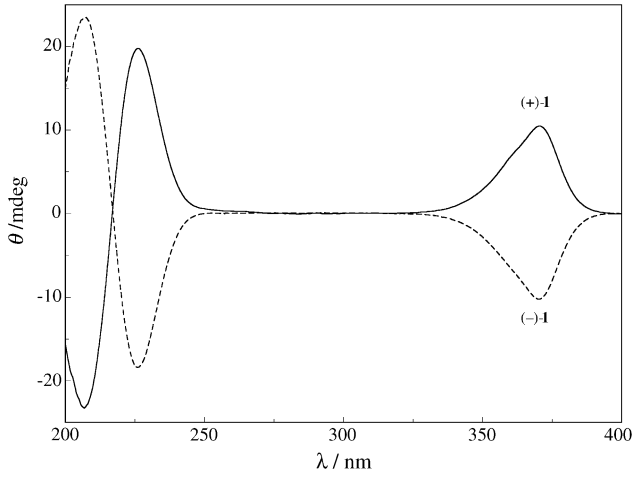

Fig. 2. Circular dichroism spectra of **1** (2 mM) in D_2O.

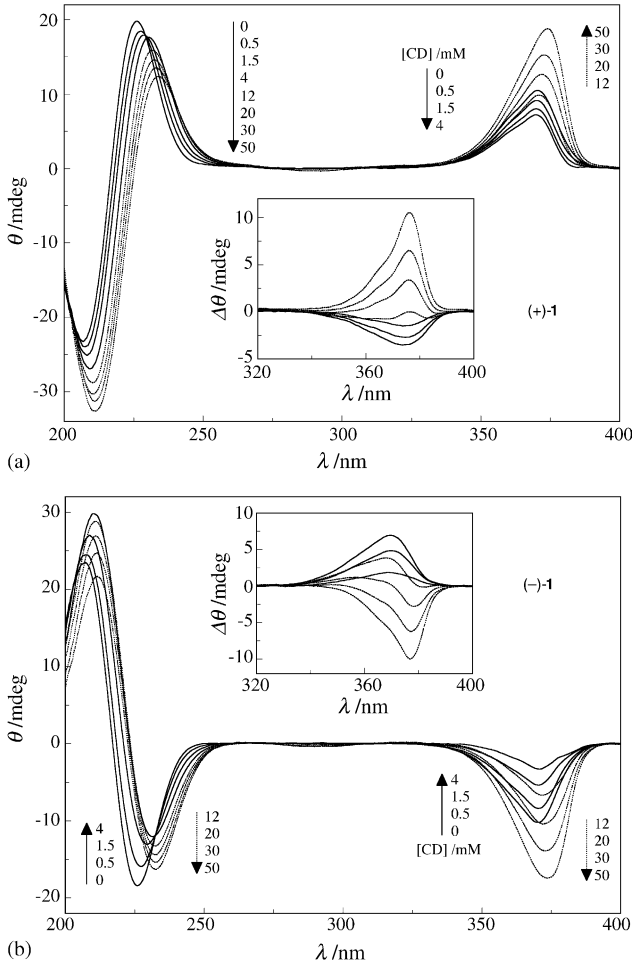

Fig. 3. Circular dichroism spectra (a) of (+)-**1** and (b) of (−)-**1** (2 mM) in D_2O at various concentrations of DMe-β-CD. The insets show the corresponding induced circular dichroism.

Fig. 3 shows the circular dichroism spectra of **1** at varying DMe-β-CD concentrations. The concentration of **1** was kept constant at 2 mM, and the circular dichroism spectra were measured at increasing DMe-β-CD concentrations from 0.2 to 50 mM. The addition of host causes highly significant and impressive effects on the circular dichroism spectra, such that we rate the information afforded by these titrations as particularly reliable. The most remarkable change in the presence of DMe-β-CD is the intensity and sign of the band peaked out at 370 nm. In the case of (+)-**1**, the addition of increasing amounts of DMe-β-CD causes first a decrease in intensity of this band and then a more pronounced increase with a red shift resulting in a maximum around 374 nm.

The effect can be corrected by subtracting the intrinsic circular dichroism effect of uncomplexed (+)-**1**. This affords the induced circular dichroism caused by complexation (inset in Fig. 3a), which reveals an down-and-up spectral feature, where the negative effect at low concentrations

can again be assigned to the circular dichroism induced in the 1:1 complex, and the positive effect to that induced in the 2:1 complex (Scheme 1, lower reaction sequence). The bathochromic shift of the band in the 2:1 complex is independently supported by the UV-spectral behavior (see above). The induced circular dichroism behavior of the (−)-enantiomer is qualitatively opposite (Fig. 3b), i.e., a positive effect is observed at low concentrations, followed by a negative effect. The spectral features in the presence of host are, however, not perfectly symmetrical to each other, since the resulting host–guest complexes are diastereomeric in nature and have slightly different structures and chiro-optic properties (in addition to opposite signs).

As predicted by the rules of Harata and Kodaka [12,44], the signs of the induced circular dichroism effects are principally suitable to provide information on the co-conformation of CD complexes with chromophoric guest, which has recently been confirmed for azoalkanes as guests [13,18,37,39]. Unfortunately, these rules have been formulated for achiral guest molecules, which lack an intrinsic circular dichroism, and they cannot be transferred in a straightforward manner to the inclusion complexes with chiral guests. The opposite induced circular dichroism for the two enantiomers is therefore unlikely to be related to orthogonal co-conformations (as would be required by the above rules). However, Kodaka's rule predicts an inversion of the sign of the induced circular dichroism when the chromophore is positioned in the same relative orientation (with respect to the CD axis) inside or outside the CD cavity. It is therefore reasonable to expect different signs when the azo chromophore is positioned outside the CD cavity (1:1 complex) or inside the CD (2:1 complex), such that the inversion of the induced circular dichroism upon populating the 2:1 complex (insets of Fig. 3) can be nicely rationalized for both enantiomers (Scheme 2).

3.3. Binding constants

The complexation-induced circular dichroism and UV-spectral changes can be used to determine the binding constants K_1 and K_2 for 1:1 and 2:1 complexation, respectively. Fitting of the titration data to the sequential complexation model requires a numerical solution (an analytical solution is not available). Several programs have been applied for specific examples [45,46], and a few general programs to solve the problem have also been described [47,48]. In the present work, we have used the cubic-equation module implemented in the program ProFit [49] to obtain reproducible and self-consistent results. In detail, the spectral changes in the UV absorbance (Eq. (1a); inset of Fig. 1) or the ellipticity (Eq. (1b); Fig. 4) were plotted against the DMe-β-CD concentration, $[CD]_0$, to afford the binding constants in Table 1. In both cases, the total concentration of the guest, $[\mathbf{1}]_0$, was held constant at 2 mM, and the titrations were performed at the wavelengths of maximum change, i.e., 370 nm for circular dichroism, and 377 nm for UV absorption; the path length (l) was 1 cm in all experiments.

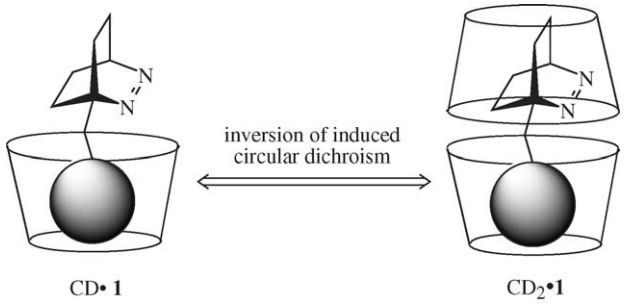

Scheme 2.

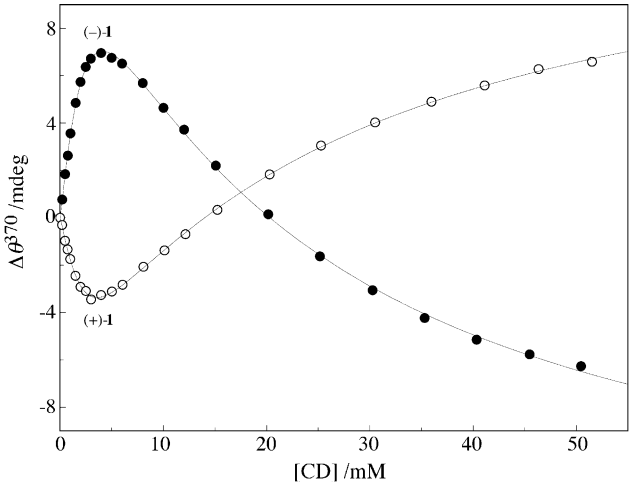

Fig. 4. Induced circular dichroism intensity titration plots (θ_{exc} = 370 nm) according to Eq. (1b); data from Fig. 3.

$$\frac{A^{\lambda}}{l} = \varepsilon_1[\mathbf{1}] + \varepsilon_{CD\cdot\mathbf{1}}[CD\cdot\mathbf{1}] + \varepsilon_{CD_2\cdot\mathbf{1}}[CD_2\cdot\mathbf{1}], \quad (1a)$$

$$\frac{\theta^{\lambda}}{32982l} = \Delta\varepsilon_1[\mathbf{1}] + \Delta\varepsilon_{CD\cdot\mathbf{1}}[CD\cdot\mathbf{1}] + \Delta\varepsilon_{CD_2\cdot 1}[CD_2\cdot\mathbf{1}], \quad (1b)$$

with

$$[\mathbf{1}] = \frac{[\mathbf{1}]_0}{1 + K_1[CD] + K_1K_2[CD]^2},$$

$$[CD\cdot\mathbf{1}] = \frac{K_1[\mathbf{1}]_0[CD]}{1 + K_1[CD] + K_1K_2[CD]^2},$$

$$\text{and} \quad [CD_2\cdot\mathbf{1}] = \frac{K_1K_2[\mathbf{1}]_0[CD]^2}{1 + K_1[CD] + K_1K_2[CD]^2}$$

[CD], the concentration of free DMe-β-CD, can be derived from the cubic equation:

$$K_1K_2[CD]^3 + K_1(2K_2[\mathbf{1}]_0 - K_2[CD]_0 + 1)[CD]^2 + (K_1[\mathbf{1}]_0 - K_1[CD]_0 + 1)[CD] - [CD]_0 = 0 \quad (2)$$

Both methods afforded a ca. 50 times higher binding constant for the formation of the 1:1 complex (K_1) than for the

Table 1
Thermodynamic, kinetic, and spectroscopic parameters for the complexation of the enantiomers **1** with DMe-β-D in D_2O under air

	(+)-**1**		(−)-**1**	
	From circular dichroism	From UV absorption	From circular dichroism	From UV absorption
Thermodynamic parameters				
K_1 (M^{-1})	1440 ± 180	1790 ± 200	1190 ± 140	1390 ± 260
K_2 (M^{-1})	36 ± 2	20 ± 2	44 ± 4	27 ± 6
K_1K_2 (M^{-2})	52000 ± 4000	35000 ± 8000	52000 ± 3000	37000 ± 15000
Kinetic parameters[a]				
k_{ass1} (10^9 M^{-1} s^{-1})	1.12 ± 0.03	0.87 ± 0.02	1.28 ± 0.06	1.12 ± 0.05
k_{ass2} (10^7 M^{-1} s^{-1})	< 1		< 1	
k_{diss1} (10^5 s^{-1})	8	5	11	8
k_{diss2} (10^5 s^{-1})	< 5		< 3	
τ_{CD_1} (ns)	220 ± 2	219 ± 1	196 ± 3	196 ± 3
τ_{CD_2} (ns)	146 ± 6	81 ± 6	190 ± 11	170 ± 14
Spectroscopic parameters				
λ_{iso} (nm)[b]		368 [372]		367 [373]
$\varepsilon_{CD_2\cdot\mathbf{1}}$ (M^{-1} cm^{-1}) [λ_{max}][c]		81 [377]		77 [377]
$\Delta\varepsilon$ (M^{-1} cm^{-1}) [λ_{max}][d]	0.21 [374]		–0.23 [374]	

[a] Determined by steady-state fluorescence quenching according to Eq. (3) by using the binding constants determined by circular dichroism or UV absorption. The dissociation rate constants were estimated by using the ground-state equilibrium constants, cf. text.
[b] Apparent isosbestic points in the UV titration; the second isosbestic point (at higher concentration) is shown in square brackets.
[c] Extinction coefficient [at the UV absorption maximum] of the 2:1 complex, extrapolated to quantitative 2:1 complexation.
[d] Molar ellipticity [at the maximum wavelength] of the 2:1 complex, extrapolated to quantitative 2:1 complexation.

2:1 complex (K_2). Although the absolute values of the two independent titration methods vary slightly, both suggest a 20% higher K_1 value for complexation of the (+)-enantiomer. The binding constants for the K_2 value show the opposite trend (larger value for (−)-enantiomer). Unfortunately, the error limits of the fitted binding constants prevent affirmative conclusions. The errors in K_1 and K_2 are also correlated, i.e., the choice of a larger value of K_1 can be compensated by a smaller value of K_2 and vice versa, which somewhat limits intuitive interpretations based on these error limits. An alternative parameter, which better reflects error-correlation, is the product of both binding constants K_1K_2, which is also listed in Table 1. We consider the binding constants obtained from circular dichroism as being more reliable than the UV data for two reasons. First, the circular dichroism titrations show a characteristic inflection point with large absolute variation (Fig. 4), which reduces the error in the fitting (in particular for the K_1K_2 product), and second, the method is insensitive to background absorption due to achiral absorbing impurities.

The binding constants K_1 and K_2 afforded by the two techniques suggest an insignificant chiral discrimination for the thermodynamics of guest binding. The diastereomeric complexes show, however, distinct spectroscopic properties, e.g., a 5% variance in the extrapolated extinction coefficients (from Eq. (1a)) and different fluorescence lifetimes (see below) of the 2:1 complexes (Table 1), which suggest a slight change of the inclusion co-conformations.

3.4. Steady-state fluorescence quenching

The DBO chromophore is quenched inside CD cavities, presumably by hydrogen atom abstraction [17,18,24], which was herein exploited to probe the kinetics of complexation of **1** with DMe-β-CD. The conceptual basis for the measurement of association rate constants by fluorescence quenching is that the singlet-excited azoalkane is sufficiently long-lived (a peculiarity of the DBO chromophore) to undergo complexation during its excited state lifetime [17,18]. The fluorescence quenching is therefore more efficient than expected from the ground-state equilibrium distribution of the complexed and uncomplexed forms alone. In other words, the fluorescence quenching is partially dynamic, and not only static, in nature, which provides a spectroscopic handle on the kinetics. Surprisingly, and in contrast to aromatic fluorescent probes, substitution of DBO shows a tendency to prolong the fluorescence lifetimes rather than to shorten them [18], and this was also the case for the camphanate derivatives **1**, which show a longer lifetime in D_2O (620 ns aerated, 840 ns deaerated, this work) than the parent DBO (505 ns aerated, 730 ns deaerated) [17,18]. The conceptual requirement of a long fluorescence lifetime is therefore fulfilled, and in fact improved.

The fluorescence quenching of DBO-type azoalkanes can be followed by time-resolved as well as steady-state fluorescence [17]. The best kinetic data can be obtained if accurate binding constants are known and if a global fitting is applied, i.e., a parallel fitting of the time-resolved and steady-state data; this has been possible for DBO derivatives showing only 1:1 complexation [18]. In the present study, we refrained from measurements of the CD-concentration-dependent time-resolved fluorescence decays (which become much more complex for a 2:1 than for the previously investigated 1:1 complexation scheme) and focused on an analysis of the steady-state fluorescence behavior. The latter can also

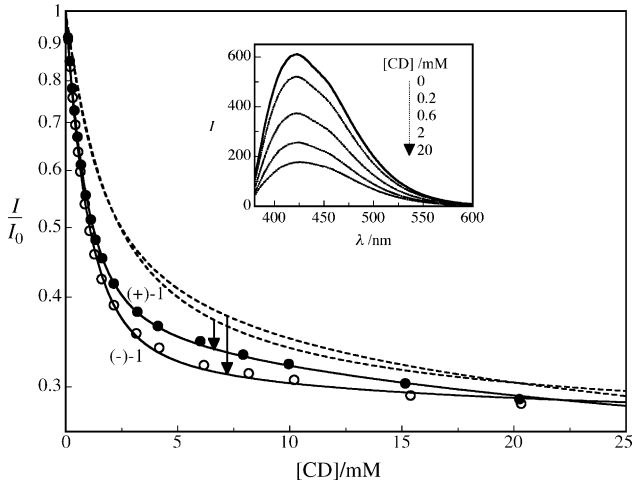

Fig. 5. Fluorescence quenching plots (λ_{exc} = 367 nm) for singlet-excited (+)-**1** and (−)-**1** in D_2O in the presence of various concentrations of DMe-β-CD and fitting according to Eq. (3); note the logarithmic ordinate scale. The dashed lines show the expected static fluorescence quenching behavior in the absence of excited-state dynamics ($k_{ass1} = 0$). The inset shows the corresponding corrected fluorescence emission spectra of (+)-**1** (0.5 mM) in D_2O at various concentrations of DMe-β-CD.

be more intuitively understood and visualized. The steady-state fluorescence titrations were performed by excitation of the azo group at 367 nm. The concentration of **1** was held constant at 0.5 mM and the concentration of DMe-β-CD was varied between 0.1 and 20 mM. The fluorescence intensity of **1** decreased gradually upon addition of DMe-β-CD, see, for example, the change of the emission spectra of (+)-**1** in the inset of Fig. 5.

The quantitative analysis is based on Scheme 1, which now includes the excited-state complexation equilibria (top). In addition, the following assumptions are made: (1) the dissociation rate constants are sufficiently small to neglect exit of the probe during its excited-state lifetime in the complexes. (2) Differences in radiative decay rates in water and CDs are small [17,43]. These two assumptions are important to derive, for the complexation sequence in Scheme 1, the following analytical expression for the steady-state fluorescence intensity ratio in the presence (I) and absence (I_0) of different CD concentrations:

$$\frac{I}{I_0} = \frac{[\mathbf{1}]}{[\mathbf{1}]_0} R + \frac{\tau_{CD_1}}{\tau_0}\frac{\varepsilon_{rel1}[CD\cdot\mathbf{1}]}{[\mathbf{1}]_0} S + \frac{\tau_{CD_2}}{\tau_0}\frac{\varepsilon_{rel2}[CD_2\cdot\mathbf{1}]}{[\mathbf{1}]_0} \quad (3)$$

with

$$R = \frac{1 + \tau_{CD_1}k_{ass1}[CD]_0 + \tau_{CD_1}k_{ass2}[CD]_0 + \tau_{CD_1}k_{ass1}k_{ass2}[CD]_0^2}{1 + \tau_0 k_{ass1}[CD]_0 + \tau_{CD_1}k_{ass2}[CD]_0 + \tau_0\tau_{CD_1}k_{ass1}k_{ass2}[CD]_0^2} \quad \text{and}$$

$$S = \frac{1 + \tau_{CD_2}k_{ass2}[CD]_0}{1 + \tau_{CD_1}k_{ass2}[CD]_0}$$

Excitation leads to the population of the fluorescent singlet-excited state of the uncomplexed **1** (**1***) with a lifetime τ_0, of the 1:1 complex (CD·**1***) with a lifetime τ_{CD_1}, and of the 2:1 complex (CD_2·**1***) with a lifetime τ_{CD_2}. The ratio depends directly on the ground-state equilibrium concentrations [**1**], [CD·**1**], and [CD_2·**1**] as obtained from Eq. (2) with the known binding constants (Table 1). In addition, the relative extinction coefficients ε_{rel1} and ε_{rel2} need to be considered to correct for differential absorption of the three species in equilibrium (Scheme 1, lower reaction sequence); the excitation wavelength was conveniently adjusted to match the first isosbestic point at 367 nm, where free **1** and its 1:1 complex absorb equally strong for both enantiomers ($\varepsilon_{rel1} = 1$), while ε_{rel2} was extrapolated from the titration fits in Eq. (1a) and afforded a value of 0.83 ± 0.03 for both enantiomers.

Due to the error statistics in photomultiplier-based fluorescence measurements, which increases with the detected fluorescence intensity (estimated as 3% in the present experiments, reproducibility) the fitting of Eq. (3) to the experimental data was performed in the logarithmic form (Fig. 5) [17]. The difference in fluorescence intensities of the two enantiomers in the region between 2 and 10 mM are experimentally significant, thus presenting an example of chiral recognition through fluorescence quenching [36]. The association rate constants k_{ass1} and k_{ass2} were extracted by a nonlinear least-squares fitting procedure along with the fluorescence lifetimes of the complexes τ_{CD_1} and τ_{CD_2} as additional fitting parameters. While the values for k_{ass1}, the rate constants for the formation of the 1:1 complex, were found to be large ($\geq 10^9\ M^{-1}\ s^{-1}$) and showed a chiral discrimination (see below), it became immediately evident that the kinetics of formation of the 2:1 complex is too slow to be significant on the time scale of the experiment (ca. 1 μs), such that only a lower limit can be provided ($<10^7\ M^{-1}\ s^{-1}$, Table 1). In other words, k_{ass2} in Eq. (3) can be set to 0 without affecting the other fitting parameters, which greatly simplifies the function (Eq. (4)).

$$\frac{I}{I_0} \approx \frac{[\mathbf{1}]}{[\mathbf{1}]_0}\left(\frac{1 + \tau_{CD_1}k_{ass1}[CD]_0}{1 + \tau_0 k_{ass1}[CD]_0}\right) + \frac{\tau_{CD_1}}{\tau_0}\frac{\varepsilon_{rel1}[CD\cdot\mathbf{1}]}{[\mathbf{1}]_0} + \frac{\tau_{CD_2}}{\tau_0}\frac{\varepsilon_{rel2}[CD_2\cdot\mathbf{1}]}{[\mathbf{1}]_0} \quad \text{for} \quad k_{ass2} < 10^7\ M^{-1}\ s^{-1} \quad (4)$$

The finding that the association rate constant for the formation of the higher-order complex falls about 2 orders of magnitude below the rate constant for 1:1 complexation (k_{ass1}; Table 1) is fully consistent with a recent finding for the rate of formation of the 2:1 β-CD–pyrene complex ($<10^7\ M^{-1}\ s^{-1}$) [34]. We propose that this kinetic feature (slower kinetics of 2:1 complex formation) is a general one. It should also be noted here that the expectation values for k_{diss1} (ca. $10^6\ s^{-1}$) and k_{diss2} ($<5 \times 10^5\ s^{-1}$), both obtained through the approximate relationship K/k_{ass} (Table 1), are too small to have a sizable influence on the kinetics [18], such that this approximation (made to derive Eq. (3), see above) can be justified, in hindsight.

Table 1 contains also the fluorescence lifetimes of singlet-excited **1** in its 1:1 complex (τ_{CD_1}) and in its 2:1 complex (τ_{CD_2}). The τ_{CD_2} values tend to be shorter, which is expected, since the chromophore is fully immersed in the 2:1 complex. However, the fluorescence lifetimes of the complexes are longer than those previously reported for 1:1 complexes of DBO with natural β-CD (<100 ns) [18]. Presumably, the quenching by DMe-β-CD is somewhat less efficient. It should be noted that there is a chiral discrimination for the fluorescence lifetimes in the 1:1 and 2:1 complexes: τ_{CD_1} was found to be longer, but τ_{CD_2} shorter for the (+)-enantiomer. Chiral discrimination on the basis of excited-state lifetimes is known, e.g., for triplet camphorquinone [41].

3.5. Kinetics of formation of the 1:1 complexes and chiral discrimination

The quintessential kinetic parameters extracted from the fluorescence quenching experiments are the association rate constants k_{ass1} for the formation of the 1:1 complexes of both enantiomers of **1**. First of all, it is important to recognize that the k_{ass1} values for **1** are larger than for smaller DBO derivatives, and lie in the upper range ($\geq 10^9\ M^{-1}\ s^{-1}$) of reported association rate constants with CDs in general [18,19,26]. Bohne and co-workers have proposed that larger association rates are promoted, among others, by a smaller size of the guest [19], while we have reached the tentative conclusion in a previous substituent effect study, that an increasing hydrophobicity increases the binding strength as well as the association rates [18]. The present result obtained for **1**, a relatively large and more hydrophobic derivative, supports the latter argument. However, differential desolvation effects due to the large structural variation must also be kept in mind [19], since it is the camphanate moiety and not the DBO moiety, which is presumably included first (Scheme 1), and therefore determines the kinetics. Finally, one must keep in mind that the presently studied CD is partially methylated, which may enhance the hydrophobicity and association rate constant for this reason, as has been suggested in a previous study [26].

Most important, our data reveal a statistically significant chiral discrimination of the kinetics of CD complex formation, i.e., $k(-) > k(+)$, regardless of whether the binding constants have been taken from either the circular dichroism or UV absorption titrations. While the discrimination is small (ca. 20%), one must keep in mind that previous attempts to manifest such a kinetic discrimination by photophysical measurements have not been successful on account of larger error limits [16]. A large effect was therefore not expected a priori, and in view of the very fast kinetics (close to the diffusion-controlled limit) large differences were also unlikely from a reactivity-selectivity standpoint. But how can there be a significant chiral discrimination on the kinetics, if the variation of the binding constants, on which the analysis of the kinetic data depends upon (see above), is not significant? The first part of the answer is that the binding constants suggest a higher or at best equally high value for (+) as for (−), cf. Table 1. The second part is that the *static* fluorescence quenching (not considering dynamic quenching by complex formation during the excited-state lifetime) would lead to a larger quenching of the enantiomer which possesses the higher binding constant, i.e., (+), since complexation leads to shorter fluorescence lifetimes. And the third part of the answer is that experimentally, i.e., by including the dynamic fluorescence quenching component, the *opposite* is observed (more efficient quenching by the (−)-enantiomer), and this deviation can only be rationalized in terms of a faster inclusion of the (−)-enantiomer. This conclusion was confirmed by monitoring the outcome of the fitting even if the extreme error limits of the binding constants were explored. For illustration, we have included in Fig. 5 (dashed lines) the expected static quenching behavior by setting $k_{ass1} = 0$ in Eq. (4). It is the discrepancy between the dashed and the solid lines for both enantiomers (the different length of the arrows in Fig. 5), which determines the significance of the kinetic chiral discrimination.

The comparison of the thermodynamic and kinetic data in Table 1 reveals that the enantiomer, which tends to show a stronger binding (+), does not show the faster rate constant for complexation, but the slower one. There appears to be no direct correlation between the thermodynamics and kinetics. Similar observations were made in previous studies of CD complexation [18,50], which points to a peculiarity of supramolecular host–guest complexation processes and emphasizes the need for additional case studies to formulate generalized trends in this area.

4. Conclusions

In summary, we have designed the novel bifunctional probe **1** for chiral discrimination by CDs, consisting of a camphanate moiety for chiral information and DBO as a spectroscopic label. DBO can be probed by UV absorption and circular dichroism to obtain information on the microenvironment of the chromophore and to determine the binding constants, while the kinetics of association can be obtained from steady-state fluorescence quenching techniques. An insignificant chiral discrimination by DMe-β-CD for the thermodynamics of 1:1 complex formation was observed, favoring the (+)-enantiomer, but a significant one for the kinetics of 1:1 complex formation, now in favor of the (−)-enantiomer. The thermodynamic and kinetic analysis of this host–guest system was complicated by the sequential formation of 1:1 and 2:1 complexes, which led to larger experimental error and more intricate fitting procedures. The application of the new probe to natural β-CD presents a future challenge, since in this case precipitation of the 2:1 complex occurs [38]. Finally, in order to obtain more impressive chiral discrimination effects on the kinetics of CD complexation, it appears imperative to choose host–guest systems with association rate constants not approaching the diffusion-controlled limit.

Acknowledgements

The authors are most grateful for financial support by the International University, Bremen. This project was funded within the NRP 47 “Supramolecular Functional Materials” by the Swiss National Science Foundation.

References

[1] J. Szejtli, Chem. Rev. 98 (1998) 1743–1753.
[2] K.A. Connors, Chem. Rev. 97 (1997) 1325–1357.
[3] M.V. Rekharsky, Y. Inoue, Chem. Rev. 98 (1998) 1875–1917.
[4] R. Breslow, S.D. Dong, Chem. Rev. 98 (1998) 1997–2011.
[5] P. Bortolus, S. Monti, Adv. Photochem. 21 (1996) 1–133.
[6] K. Uekama, F. Hirayama, T. Irie, Chem. Rev. 98 (1998) 2045–2076.
[7] K. Takahashi, Chem. Rev. 98 (1998) 2013–2033.
[8] S. Li, W.C. Purdy, Chem. Rev. 92 (1992) 1457–1470.
[9] H.J. Schneider, F. Hacket, V. Rüdiger, H. Ikeda, Chem. Rev. 98 (1998) 1755–1785.
[10] H. Dodziuk, W. Kozminski, A. Ejchart, Chirality 16 (2004) 90–105.
[11] K. Harata, Chem. Rev. 98 (1998) 1803–1827.
[12] K. Harata, H. Uedaira, Bull. Chem. Soc. Jpn. 48 (1975) 375–378.
[13] X. Zhang, W.M. Nau, Angew. Chem. Int. Ed. 39 (2000) 544–547.
[14] S. Allenmark, Chirality 15 (2003) 409–422.
[15] F.P. Schmidtchen, Chem. Eurr. J. 8 (2002) 3522–3529.
[16] T.C. Barros, K. Stefaniak, J.F. Holzwarth, C. Bohne, J. Phys. Chem. A 102 (1998) 5639–5651.
[17] W.M. Nau, X. Zhang, J. Am. Chem. Soc. 121 (1999) 8022–8032.
[18] X. Zhang, G. Gramlich, X. Wang, W.M. Nau, J. Am. Chem. Soc. 124 (2002) 254–263.
[19] M. Christoff, L.T. Okano, C. Bohne, J. Photochem. Photobiol. A: Chem. 134 (2000) 169–176.
[20] S. Petrucci, E.M. Eyring, G. Konya, in: J.L. Atwood (Ed.), Comprehensive Supramolecular Chemistry, Elsevier, Oxford, 1996, pp. 483–497.
[21] M.H. Kleinman, C. Bohne, in: V. Ramamurthy, K.S. Schanze (Eds.), Molecular and Supramolecular Photochemistry, Marcel Dekker Inc., New York, 1997, pp. 391–466.
[22] F. Cramer, W. Saenger, H.-C. Spatz, J. Am. Chem. Soc. 89 (1967) 14–20.
[23] S. Nishikawa, N. Yokoo, N. Kuramoto, J. Phys. Chem. B 102 (1998) 4830–4834.
[24] S. Monti, L. Flamigni, A. Martelli, P. Bortolus, J. Phys. Chem. 92 (1988) 4447–4451.
[25] M. Barra, C. Bohne, J.C. Scaiano, J. Am. Chem. Soc. 112 (1990) 8075–8079.
[26] L.T. Okano, T.C. Barros, D.T.H. Chou, A.J. Bennet, C. Bohne, J. Phys. Chem. B 105 (2001) 2122–2128.
[27] C. Bohne, Spectrum 13 (2000) 14–19.
[28] M. Ghosh, R. Zhang, R.G. Lawler, C.T. Seto, J. Org. Chem. 65 (2000) 735–741.
[29] C.T. Yim, X.X. Zhu, G.R. Brown, J. Phys. Chem. B 103 (1999) 597–602.
[30] Y. Kotake, E.G. Janzen, J. Am. Chem. Soc. 114 (1992) 2872–2874.
[31] M. Lucarini, B. Luppi, G.F. Pedulli, B.P. Roberts, Chem. Eur. J. 5 (1999) 2048–2054.
[32] N. Yoshida, J. Chem. Soc., Perkin Trans. 2 (1995) 2249–2256.
[33] A. Abou-Hamdan, P. Bugnon, C. Saudan, P.G. Lye, A.E. Merbach, J. Am. Chem. Soc. 122 (2000) 592–602.
[34] A.S.M. Dyck, U. Kisiel, C. Bohne, J. Phys. Chem. B 107 (2003) 11652–11659.
[35] K.N. Houk, A.G. Leach, S.P. Kim, X. Zhang, Angew. Chem. Int. Ed. 42 (2003) 4872–4897.
[36] L. Pu, Chem. Rev. 104 (2004) 1687–1716.
[37] B. Mayer, X. Zhang, W.M. Nau, G. Marconi, J. Am. Chem. Soc. 123 (2001) 5240–5248.
[38] H. Bakirci, W.M. Nau, J. Org. Chem. 70 (2005) 4506–4509.
[39] H. Bakirci, X. Zhang, W.M. Nau, J. Org. Chem. 70 (2005) 39–46.
[40] V. Balzani, A. Credi, F.M. Raymo, J.F. Stoddart, Angew. Chem. Int. Ed. 39 (2000) 3348–3391.
[41] P. Bortulus, G. Marconi, S. Monti, B. Mayer, J. Phys. Chem. A 106 (2002) 1686–1694.
[42] C. Marquez, W.M. Nau, Angew. Chem. Int. Ed. 40 (2001) 4387–4390.
[43] J. Mohanty, W.M. Nau, Photochem. Photobiol. Sci. 3 (2004) 1026–1031.
[44] M. Kodaka, J. Phys. Chem. A 102 (1998) 8101–8103.
[45] H. Fujiwara, F. Sakai, Y. Sasaki, J. Phys. Chem. 83 (1979) 2400–2404.
[46] D.M. Kneeland, K. Ariga, V.M. Lynch, C.-Y. Huang, E.V. Anslyn, J. Am. Chem. Soc. 115 (1993) 10042–10055.
[47] M.J. Hynes, J. Chem. Soc., Dalton Trans. (1993) 311–312.
[48] A.P. Bisson, C.A. Hunter, J.C. Morales, K. Young, Chem. Eur. J. 4 (1998) 845–851.
[49] ProFit 5.6.3 ed., QuantumSoft, Zürich, Switzerland.
[50] Y. Liao, C. Bohne, J. Phys. Chem. 100 (1996) 734–743.